An Optimization Framework for Planning Wayside and On-board Hybrid Storage Systems for Tramway Applications

Authors: Marcos Tostado-Véliz, Paul Arévalo, Francisco Jurado

Keywords: Tramway, Battery energy storage, Super-capacitor, Mixed integer linear programming, Data reduction

Nomenclature

Superscripts

BES	Battery energy storage
SC	Super-capacitor
HES	Hybrid energy storage
ch/dch	Charging/discharging
TW	Tramway
G	Grid
D	Dissipated
$\overline{(\cdot)}$	Maximum value of a variable or parameter

Indices (Sets)

$y(\mathcal{Y})$	Year
$t(\mathcal{T})$	Time
$j(\mathcal{J})$	Battery technology
$r(\mathcal{R})$	Representative roundtrip

Parameters

v, q	Pair of points for Adaptive Piecewise Constant Approximation of a time series C (-)
k	Inflation rate (pu)

ω	Total roundtrips completed by the tramway per day (-)
κ	Capital costs of storage section ($/kWh)
π	Power conversion system and balance of plant costs ($/kW)
ν	Replacement costs ($/kW)
μ	Fixed operation and maintenance (O&M) costs ($/kW-yr)
ξ	Variable O&M costs ($/MWh)
ρ	Energy density (Wh/kg)
γ	If equals to 1, indicates that an element has to be replaced (Binary)
τ	Time step (hrs)
ϱ	Self-discharge rate (pu/day)
λ	Electricity cost ($/kWh)
ϑ	Energy-to-power ratio (hrs)
L	Large positive number (-)
η	Efficiency (pu)
d	Depth of discharge (pu)
Ψ	Budget limit ($)
M	Weight limit (kg)
$\mathbf{c} \in \mathbb{B}^{\mathcal{T}}$	It models sections with or without catenary (1 if the tramway can be supplied from catenary at time t, 0 otherwise)
Δ	Maximum power variation in 1 second (pu) - virtual ramp

Decision variables

Q	Storage capacity (kWh)
$\overline{p}$	Nominal power of storage assets (kW)
p	Power (kW)

s	Energy stored (kWh)
u	Commitment status (Binary)
y	Dummy variable (kW or binary)

Abstract: electric mobility is gaining importance on pursuing decarbonisation of transport sector. In this context, electric tramways are recognised as a clean urban collective conveyance. Strong evidences manifest the advantages of storage systems in tramway applications. Despite its apparent benefits, the planning of such kind of systems for tramway applications has received few attention in literature. This work aims at filling this gap. To this end, a novel optimization framework for planning hybrid storage systems (batteries + super-capacitors) for tramway applications on either wayside or on-board configurations is developed, which incorporates an energy management tool to effectively coordinate the different storage technologies. Specific issues related with high resolution tramway demand measurements are addressed by using data dimensionality reduction techniques and temporal representation by representative trips. The new proposal is validated for a real Cuenca - Ecuador tramway for which extensive simulations are carried out with different storage system layouts (super-capacitors, super-capacitors + batteries), and configurations (wayside and on-board) including different electrochemical batteries technologies (lead-acid, nickel cadmium and lithium ion). The results obtained show the benefits of storage systems in tramway facilities (in fact, the total cost of the project can be reduced by 71%), highlighting the importance of fast-acting technologies such as super-capacitors to handle high peak demand consumptions, while batteries are primarily dedicated to providing backup long-term storage capacity. Wayside and on-board configurations are also compared, revealing that total weight of the storage system suppose the main barrier for large capacity installation in on-board layouts.

1- Introduction

1.1. Context and Motivation

Energy storage systems in tramway applications aim to increase energy efficiency through adequate energy planning and control. Typically, storage systems for tramway installations encompass batteries and super-capacitors (SCs) [1-3]. Stationary battery energy storage (BES) systems compared to other technologies improves traction efficiency and reduces associated costs, reaching savings rate of up to 25% [4-6]. SCs are useful in traction applications because their high power density, long useful life, low maintenance costs and specifically short charge/discharge times [7]. In contrast, electrochemical batteries such as lead acid, lithium ion (Li-ion) and nickel cadmium (Ni-Cd), have high energy density being able to store energy from regenerative braking [8]. In this way, both storage technologies combine their characteristics getting a more efficient energy management of the system. Real projects at Long Island, London and Madrid have evidenced the effectiveness of hybrid energy storage (HES) systems to notably improve the efficiency of tramway installations [9-11].

Despite the apparent importance of HESs in tramway applications, existing literature is mainly focused on operational tools, while planning stages have been traditionally ignored or simplified. Planning tools for HESs in tramway applications require a complementary effort with respect to other related instruments. Thus, specific issues such as high time resolution of measurements and diversity of storage technologies need to be addressed by developing specific tools. This paper aims to fill this gap.

1.2. Literature review

Due to the salient features demonstrated by HES systems in tramway applications, such installations have received great attention for their energy, economic and environ-

mental feasibility [12-14]. As commented, HES systems for tramway applications normally encompass batteries and SCs. In [12], the authors proposed a model predictive control scheme for optimal coordination of batteries and SCs in light rail vehicles. The authors in [14] focused on the importance of storage systems in tramway applications to store the energy generated during braking. This way, braking energy can be stored rather than dissipated in order to boost up the efficiency of the installation. In [15], a comparison of a tramway system without energy storage and a tramway equipped with Li-ion batteries was performed. In this case, only wayside configuration was analyzed while the possibility of on-board installation was not contemplated. The results revealed that the payback time may be reduced from 6 years to 4.5 years if a battery storage system is installed. In [16], a catenary supplied HES system formed by batteries and SCs was studied, the authors discussed an optimal strategy combined with fuzzy logic for an HES system that supplies a tramway. The results evidenced the ability of the proposed strategy to reduce the daily operational costs by 14.6%, thus increasing the overall efficiency of the system.

Alternative storage technologies such as fuel-cell/electrolyzers groups have recently gained attention for tramway installations. The group of references of Torreglosa, et al, (e.g. see [17, 18]) is a clear example of this trend. In these references, a fuel-cell/battery/SC tramway installation is deeply analyzed. Different management strategies such as predictive control algorithms were proposed for controlling the electronic interfaces in order to achieve an adequate state of charge (SOC) management of the storage assets. A real case study served to demonstrate the suitability of predictive control for tramway applications. Moreover, the results evidenced that traction load can be effectively supplied from the storage system, reducing the dependency of external sources while the DC bus voltage is kept constant at 750 V and SOCs are maintained about the desired values.

Other strategies were more focused on reducing voltage fluctuations and other undesirable transient phenomena. To this end, energy management strategies based on adaptive droop control [19], self-convergence droop [20] and machine learning [21], have been studied. Various case studies served to prove the effectiveness of such control schemes to maintain the catenary voltage stable by controlling the SOC and power ranges of each component. Similarly, Flavio Ciccarelli et al [22], presented a control strategy for energy management of a storage system with SC in wayside configuration. The main objective was regulating the voltage in the catenary in order to optimize the power flow between the tramways and the substations installed throughout the route. These strategies are used to obtain optimal performance by addressing the highly fluctuating load demand between different power sources in the hybrid system. Pursuing the same goal, the authors of [23] developed a master-slave control strategy for a tramway installation equipped with a proton-exchange-membrane fuel cell storage system, revealing the capability of this control scheme to maintain the components voltage within security ranges avoiding fast degradation of devices.

The references above, however, start from a predefined sizing of the HES system. This assumption is quite unrealistic and optimal planning tools are necessary during designing stages to optimally determine the capacity of the different components. Few exceptions exist in the literature that clearly address the optimal sizing of storage assets for tramway applications. Specific problems in these installations such as high resolution data hinder the applicability of analytic optimization methods because computational intractability issues. As a sake of example, power profiles of tramway loads usually need a resolution of ~1s to capture fast peak periods. This data resolution entails a very high computational burden if analytic optimization techniques are employed. This issue has motivated the usage of metaheuristic methods in [2, 3, 13]. These references presented an

optimal energy management and sizing strategy for a light rail vehicle with an on-board storage system comprising batteries and SC. The authors used a multi-objective optimization approach which is solved using genetic algorithms. Along the disadvantages of using metaheuristic methods instead of analytic techniques [24], the proposed approach presents various additional drawbacks. In this sense, only one roundtrip is considered, which importantly limits the applicability of this method in for example dynamic energy pricing paradigms. Only Li-ion batteries are contemplated and other important simplifications assumed, for instance, the energy management strategy is predefined rather than optimized. In other words, the operational costs of the installation are determined on the basic of heuristic rules thus inevitably oversizing the different components since the result obtained is sub-optimal.

The limitations of the methodology in [2, 3, 13] have motivated multiple efforts from alternative point of views. For example, other authors simply encompass the traction load within a holistic planning tool in which the storage components are optimized alongside other microgrid generators such as wind turbines. In such cases, high resolution data of power traction load is further simplified in order to be properly treated. In order to keep the mode tractable and thus including a variety of uncertainties such as solar generation, traction load is frequently roughly simplified, which may entail accuracy issues. In addition, this kind of approaches normally oversimplify the storage system planning, ignoring important aspects such as cycling aging of batteries. Mohammad Hemmati, et al, [25], studied an optimal programming problem for microgrid based on economic and environmental viewpoint. Ahmad Ghasemi, et al, [26] proposed a risk-based optimization framework to determine retail electricity prices. The method considers the uncertain generation of renewable energy sources and the estimated hourly prices of the wholesale electricity market, revealing a decrease in the expected cost and the peak value of the demand by

24.63% and 5.92%, respectively. It is worth mentioning that the main advantage of microgrid planning is the ability to reduce operating cost considering the stochastic behavior of renewable sources [27, 28].

1.3. Novelty and contributions

This paper is motivated in various important gaps encountered in the related literature. In our opinion, planning of specific HES systems for tramway applications present various challenges that have not been properly addressed yet. For the sake of simplicity, the main literature gaps that aim to be filled in this work are listed below:

- Most of the related literature is focused on operational algorithms rather than planning stages. In this context, the storage system is supposed to be predefined and its design ignored.
- In most cases, only one battery technology is considered. This simplification may be unaffordable in HES systems, as pointed out in [29].
- The few planning tools used in tramway applications have limited applicability. This is mainly due to intrinsic high data resolution of power traction profiles, which usually entails computational intractability issues. To circumvent such issue, heuristic foundations have been mainly assumed, which inevitably lead to sub-optimal solutions.
- Most of the related literature assumes the storage system installed either wayside or on-board. This assumption hinders the possibility of comparing both constructive solutions, which may result valuable in real life applications.

This paper aims to solve the limitations and gaps exposed above. To this end, a Mixed-Integer-Linear programming (MILP) model for optimal planning of HES systems for tramway applications is developed. The developed technique presents various advantages

compared to other existing approaches. More precisely, the main contributions of this paper are listed below.

- Developing a MILP framework for optimal HES system layout design for tramway applications. Because its MILP formulation, the developed method is modular and solvable using analytic techniques and commercial solvers [30]. These features make the adopted solution very useful in real life applications, being capable to be adapted to different installations and situations.
- To reduce the amount of data to be treated, an original approach is proposed by which the daily tramway route is represented by means of representative roundtrips. The proposed representation allows to reduce the amount of roundtrips that are considered in simulations, without losing capability of incorporating dynamic energy pricing. Also, the proposed methodology enables a coherent representation of the SOC of the different components.
- The approach above is combined with data dimensionality reduction techniques, by which the resolution of the power tramway profiles can be reduced without losing accuracy. By this approach, the problem is computationally tractable using average machines, promoting the universal applicability of the developed methodology.
- The developed MILP model allows to contemplate as many storage technologies as considered. Also, simplifications on cycling and calendric aging of storage components are not assumed.
- The developed model is applicable to on-board and wayside configurations, thus allowing a fair comparison between the two solutions.
- The developed optimization problem considers the capacity and rated power of storage components as independent variables. This way, both the storage capacity

and energy-to-power ratio are independently optimized, as occurred in real life situations.

A case study based on a real tramway installation at Cuenca (Ecuador) has been considered. Various simulations and results are presented to prove the effectiveness and accurateness of the developed approach. This case study serves to validate the developed approach for real life applications along to analyze the role of HES systems in tramway installations.

The remainder of the paper is organized as follows, section 2 describes the developed methodology. The mathematical formulation of the developed MILP optimization framework is presented throughout section 3. Several results on a real tramway installation are provided and analyzed in section 4. This paper is concluded with section 5.

2 - Developed Methodology

2.1 - System overview

The tramway system under study encompasses various components such as shown in Fig. 1. It is assumed that the traction load is supplied from an overhead catenary which is stocked from a DC substation. In this regard, the catenary acts as a primary energy supply while a hybrid storage system complements it. The storage bank can be installed wayside or on-board. In the first case, the storage system supplies the tramway through the catenary, while in the latter it directly provides energy to the traction machinery. In both cases, the storage system is formed by SCs and batteries, as customary in tramway installations (e.g. see [20, 23]). SCs are mainly devoted on supplying fast peak loads produced by the tramway during acceleration, while the battery energy storage (BES) system provides large storage capacity [23]. In both cases, DC-DC converters are installed to properly operate the storage devices as well as keep catenary voltage constant [20]. Modern electric tramways incorporate regenerative braking. In this regard, tramway motors work in

generator mode during braking producing energy that can be either stored or dissipated on braking resistors.

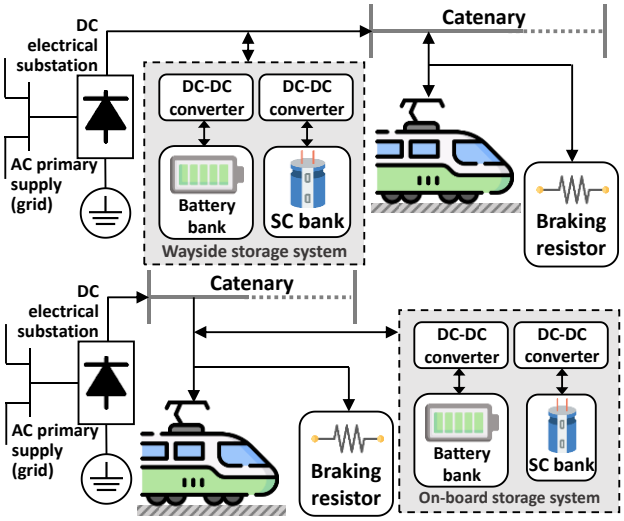

Fig. 1 - Pictorial representation of the tramway system under study with wayside (upper) or on-board (bottom) energy storage system comprising batteries and SCs

Henceforth, it is assumed that energy scheduling of the system in Fig. 1 is centralised determined by a management system. Such frameworks are very popular in modern energy systems such as microgrids (e.g. see [31]). In essence, an energy management system decides the scheduling plan of the different assets over a determined time horizon in order to accomplish a series of imposed objectives. Conventionally, the energy management frameworks aim at fulfilling the demand at minimum cost. By applying this idea to the tramway system under study, the entire traction load must be supplied reducing the energy purchased from the grid. In this context, it is assumed that any kilowatt-hour supplied from the DC substation has a known cost. The energy management algorithm is essential on the developed methodology as it determines the daily costs of the system. It is worth mentioning that many power/energy management systems have been proposed for tramway applications (see Introduction). However, such approaches are rather devoted on controlling electronic interfaces under real-time conditions, while the energy management concept presented in this paper is rather devoted on the task scheduling problem. Due to this feature, the approach that has been presented in this study can be conceived

as the application of the home appliances scheduling concept [32] to tramway installations. The energy management system considered for the system of Fig. 1 and its mathematical formulation are further explained in Section 3.

2.2 - Overview of the developed methodology

The main aim of this work is to develop a methodology for comprehensive planning hybrid storage systems for tramway applications. To this end, a MILP optimization framework has been developed which is fully described in Section 3. The formulation of such optimization problem involves a series of costs which are evaluated over different time horizons. Thus, while capital costs are evaluated once during the project lifetime, other expenditures have to be assessed over yearly or daily time horizons. In this sense, while capital and yearly costs are determined by the different components sizing, the daily expenditures are mainly influenced by the control strategy adopted by the simulated energy management algorithm. For this purpose, the tramway demand curve during a roundtrip has to be provided. This information can be obtained from real measured data or determined by the well-known speed-power curves [20] and the slope profile of the route [33]. Demand curve for tramway applications should present a very high resolution (~1s [34]), in order to accurately capture fast peak load consumptions. This requirement provokes that a huge amount of data have to be treated, which may make the optimization problem intractable in practise. To solve this issue, this paper proposes to take advantage that daily demand of a tramway installation is conventionally quite repetitive and it can be well described by the power curve of only one roundtrip [33]. Even so, the amount of data may be still quite large. Indeed, a complete tramway roundtrip may take up to 1 hour. This way, if a resolution of 1s is required, the variables of the problem would have 3,600 dimensions, which may suppose intractability issues. To circumvent this issue, it is pro-

posed to reduce the resolution of the power curve by using the Adaptive Piecewise Constant Approximation (APCA) [35]. Component costs, expected project lifetime and inflation rate are also assumed to be known data. All this information is provided to the developed MILP framework on the form of parameters. The developed methodology not only yields the optimal configuration of the hybrid storage system, but also other valuable results such as the expected project cost, total energy dissipated on the braking resistor, etc. For the sake of summarizing, Fig. 2 presents a flowchart of the developed methodology.

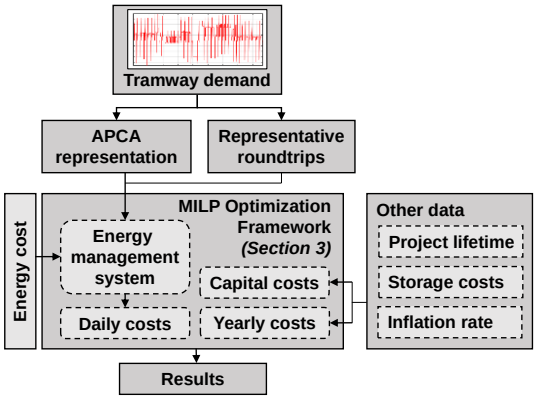

Fig. 2 Flowchart of the developed methodology for optimal sizing HES systems in tramway installations

2.3 - Time horizon representation by means of representative roundtrips

As seen in Fig. 2, the developed methodology starts from a known tramway demand profile. As commented, this data typically requires a high time resolution to capture the fast dynamic of tramway installations. Nevertheless, the daily tramway demand typically shows a repetitive pattern. This idea is quite intuitive since tramway roundtrips are almost identical. Thereby, the traction load it also expected to be quite similar. This is confirmed by analysing some real cases. The urban tramway installation placed at Cuenca, Ecuador, which is analysed in [33], is a clear example. It can be checked in this reference that real measured data of traction load for this installation is quite repetitive. In this paper, it is proposed to exploit this feature in order to reduce the amount of data to be treated. This way, one could think that only one roundtrip may be sufficient to simulate the energy

management algorithm of a tramway installation. However, this assumption may be too simplistic and some relevant aspects might not be properly analysed. Indeed, the lonely consideration of one roundtrip cannot effectively deal with dynamic energy pricing rates. On the other hand, the SOC of the storage system could not be coherently represented by just one roundtrip [24]. Indeed, if one only considers one roundtrip, the initial and final SOCs of the storage assets should be fixed at the end and beginning of the trip. Due to a tramway roundtrip usually takes few hours [33], this restriction may provoke inaccuracies to represent the charging-discharging daily pattern of the storage devices.

To overcome the issues above, it is proposed to represent the time horizon by means of representative roundtrips rather than just considering the demand of one route. This idea is pictorially illustrated in Fig. 3. As seen in this figure, daily roundtrips are divided into representative sets (which are denoted by r and conform the set $\mathcal{R}$). The most obvious way to divide the daily roundtrips is putting attention on the energy cost. Fig. 3 shows an example in which a typical dynamic pricing rate divided in two periods (peak and off-peak) is illustrated. Intuitively, this pricing scheme can be effectively represented by two sets of roundtrips. However, further divisions are necessary for handling with the daily SOC profile of the storage system. Considering the example of Fig. 3, if only two round-trips are taken, the SOC among roundtrips is over restricted. Of course, one can still think that the time horizon can be divided as many times as roundtrips are completed each day. However, advantages from data reduction are lost if this approach is considered. There are not formal rules to select the number of representative roundtrips and the adoption may vary depending on the degree of accurateness desired. Nevertheless, in this paper the rules listed below are adopted:

- The first and last roundtrips are themselves representative roundtrips. Then, the final SOC of the last roundtrip is taken equal to the initial SOC of the first roundtrip. This way, it is ensured that the SOC at the beginning and the end of the day are equal, as customary in energy management problems [24]. In addition, the initial SOC of the last roundtrip should be equal to the final SOC of the previous trip. These sets correspond with $r = 1$ and $r = 5$ in Fig. 3.
- Time horizon is then divided as many times as different pricing rates exist. Then, each roundtrip would lie within its corresponding set, according to the energy cost observed during its course. These sets correspond with $r = 2$ and $r = 4$ in Fig. 2 for the off-peak and peak pricing rates, respectively. As seen in this figure, the initial SOC of these sets should be equal to the final SOC of the previous roundtrip.
- Variation of energy pricing may have a direct impact on the charging-discharging behaviour of a storage system [24]. For instance, off-peak hours are frequently exploited for charging the storage bank in order to posteriorly discharge it during peak hours. Thus, a more economical management of the system is normally achieved. In order to properly reflect this behaviour, those roundtrips that precede a change on the energy cost are considered as representative themselves. This corresponds with $r = 3$ in Fig. 3. As seen in this figure, the initial SOC is equal to the final SOC of the previous roundtrip. However, the final SOC is a free parameter.

As mentioned, the rules above are only indicative and other approaches could be taken for convenience. It is worth remarking the relationship between the initial and final SOCs of each representative roundtrip, which are denoted by discontinuous green lines in Fig. 3.

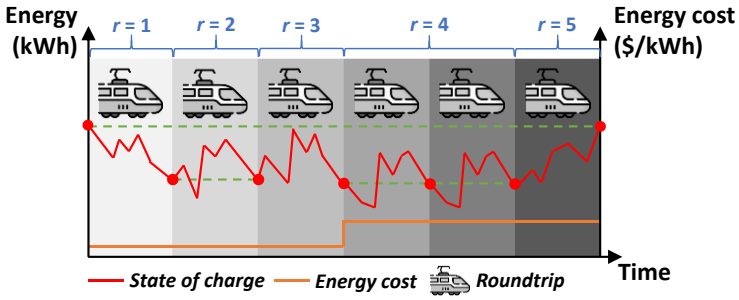

Fig. 3 Illustration of the approach considered to represent the time horizon by means of representative roundtrips

2.4 - APCA representation

As commented, typical fast peak tramway consumptions require a very high resolution sampling time (~1s) to be properly represented. This supposes that a huge amount of data has to be mathematically handled, which may result in intractability problems. To solve this issue, one can use a well-known dimensionality reduction technique. More precisely, the APCA algorithm [35] has been used in this paper. This technique is an evolution of the Piecewise Aggregate Approximation (PAA) method [36]. The fundamentals of the APCA technique are pictorially represented in Fig. 4. Given a time series $C = \{c_1, \dots, c_n\}$, the APCA representation of C is defined as follows:

$$C = \{\langle v_1, q_1\rangle, \dots, \langle v_m, q_m\rangle\}; \text{with } m \leq n \tag{1}$$

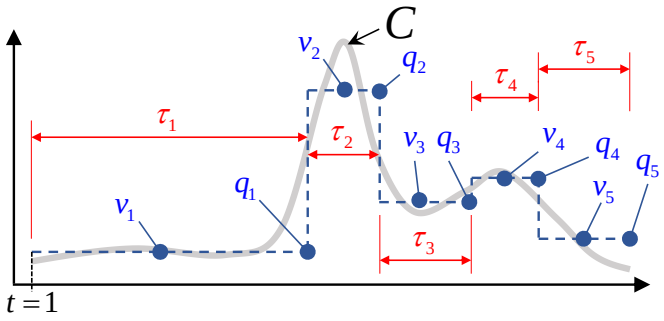

Fig. 4 Sketch of the APCA representation of a generic time series C

As seen in Fig. 4, the APCA representation of C consists on dividing it into m segments, which are fully described by its average value v and right endpoint q. As pointed out in (1), size of the APCA representation is typically quite smaller than that of the original series. This undoubtedly supposes a dimensionality reduction of the original signal,

which is reflected on a notable reduction of the data to be treated. In contrast to PAA, size of the segments can be taken variable, which supposes a valuable advantage compared with PAA and makes it very suitable for tramway applications, since traction demand typically presents a quite characteristic pattern formed by periods of almost constant demand during cruise, followed by fast peak demand periods produced by acceleration and braking. Indeed, a large segment may be used for those periods in which the demand is almost constant while very short segments could be considered for fast load variations. This is the main reason why the APCA technique has been preferred in this work instead of other methodologies.

Obviously, dimensionality reduction of C into m segments should not be performed heuristically. In this sense, it is said that that a m-segment representation is optimal if C has the least reconstruction error among all possible m-segment APCA representations. The task of finding the optimal m-segment representation of a time series is a dynamic programming problem with computational cost $O(m \cdot n^2)$ [37]. This computational burden may suppose a barrier especially in large time series. To overcome this issue, an efficient algorithm was proposed in [38], which is summarized in Fig. 5. Although this method does not generally achieve the optimal m-segment representation of C, the computational cost reduction to $O(n \cdot \log(n))$ compensates this drawback since this procedure often yields an acceptable APCA reduction in terms of accurateness. This algorithm works by firstly converting the problem into a Haar discrete Wavelet compression one. To do that, the original series is represented by Haar coefficients, which are recursively calculated for different levels of resolution l. Once this task has been performed, it is necessary to determine which coefficients are retained in order to achieve a near optimal APCA representation of C. There are multiple ways to do this; for instance, in [40] the authors proposed to take the largest m coefficients, considering m a parameter to be

tuned. However, this approach still presents some heuristic degree on the deciding the value of m. To circumvent this problem, various thresholding approximations have been proposed in the literature. For example, the GitHub repository of the algorithm in Fig. 5 [39] incorporates a universal [40] and a sub-band specific [41] thresholding approaches, and the user can select one or another for convenience. Any case, the different Haar coefficients have to be previously scaled by divided them by $2^{l/2}$. The last steps of this algorithm consist on reconstructing the series. This is necessary since the segments in the reconstructed signal may have approximate mean values. Thus, they are replaced by the exact mean values in the last stage. By the algorithm explained above, the tramway demand is no longer described by a high resolution time step, instead, the signal is replaced by APCA information, as follows

$$p_t^{\mathrm{TW}} = v_t;\ \forall t \in \mathcal{T} \tag{2}$$

where size of $\mathcal{T}$ is m.

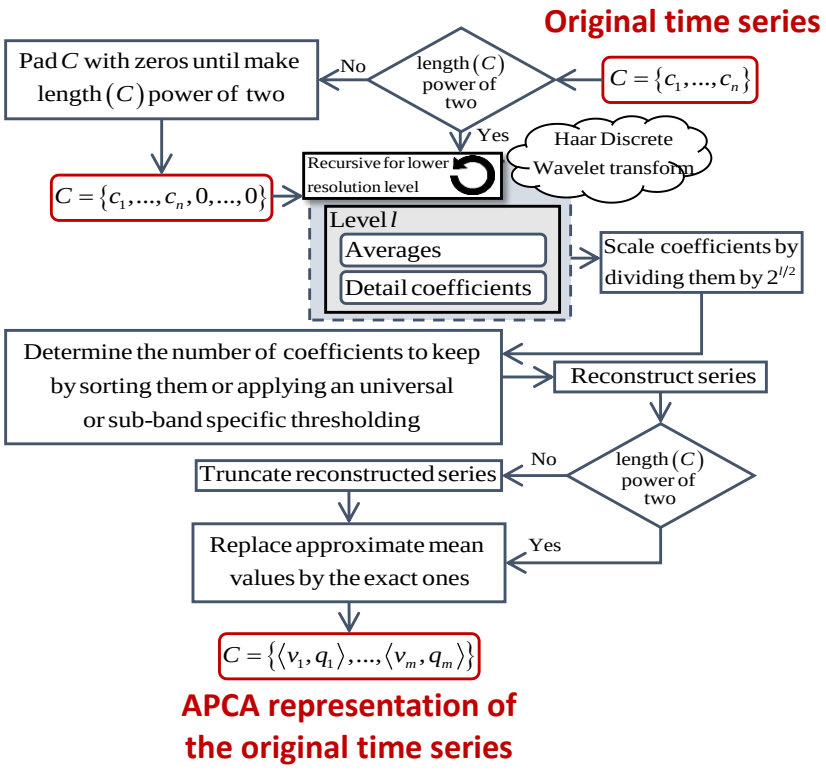

Fig. 5 Flowchart of the algorithm proposed in [37] for efficient APCA representation of a time series C

It is worth remembering that both representative roundtrips and APCA representation of the tramway demand are approaches that are considered necessary to efficiently manage the traction load data by an energy management algorithm, in order to determine the daily costs of the tramway installation under study. In this sense, energy management problems are conventionally carried out over a predetermined time horizon which is discretized on time steps. In this regard, the value of the time step is essential for the accurateness of the solution [31]. The time step is usually taken fixed for simplicity, however, this approach is not valid when an APCA approximation is considered. This issue is clearly illustrated in Fig. 4. As seen in this figure, time steps (which are represented in this figure as τ's) are not constant due to segment size is not constant either. To this end, it is proposed to take a variable step size, which can be determined any time instant by the information yielded by the APCA technique, as follows

$$\tau_t = \begin{cases} q_t, & t = 1 \\ q_t - q_{t-1}, & t > 1 \end{cases}; \ \forall t \in \mathcal{T} \tag{3}$$

3 - Mathematical formulation of the planning problem

3.1 - On the aging of storage system

It is well-known that lifetime of a storage system is determined by its calendric and cycling aging [29, 42]. The former has influence even if the storage facility is not exploited, whereas the latter is provoked by the total number of charging-discharging cycles completed over a time horizon. In the developed MILP model, cycling aging is considered by introducing a variable maintenance term for the storage units in the objective function. Thereby, replacement cost is considered only when a component has surpassed its expected lifetime and has to be replaced. However, a storage device may need to be replaced earlier due to cycling aging. To properly consider this factor in the developed mathematical framework, an iterative solution procedure is proposed, by which the problem is

firstly solved ignoring cycling aging of components. After obtaining a solution, the energy management part of the MILP optimization problem allows to calculate the total charging-discharging cycles completed by the different storage facilities through project lifetime. This way, one can check if a component needs to be earlier replaced due to cycling aging. If so, the objective function is rearranged (modifying the value of the parameter γ) and the problem is repeated. This procedure is iteratively running until the objective function faithfully reflects the aging of components, taking the last solution as the optimal planning result.

3.2 - Objective function

The developed planning tool aims at determining the optimal storage system layout. Therefore, the objective function of the developed optimal sizing problem is given by:

$$\min_{\Phi} K + \sum_{\forall y \in y}\left\{(1+k)^{y-1} \cdot \left(Y_y + 365 \cdot \sum_{\forall r \in \mathcal{R}}\{\omega_r \cdot D_r\}\right)\right\} \quad (4)$$

where K, Y and D are the capital, yearly and roundtrip costs, respectively, which are calculated as:

$$K = \sum_{\forall j \in \mathcal{J}}\left\{Q^{\mathrm{BES},j} \cdot \kappa^{\mathrm{BES},j} + \bar{p}^{\mathrm{BES},j} \cdot \pi^{\mathrm{BES},j}\right\} + Q^{\mathrm{SC}} \cdot \kappa^{\mathrm{SC}} + \bar{p}^{\mathrm{SC}} \cdot \pi^{\mathrm{SC}} \quad (5)$$

$$Y_y = \sum_{\forall j \in \mathcal{J}}\left\{\bar{p}^{\mathrm{BES},j} \cdot \left(\gamma_y^{\mathrm{BES},j} \cdot \nu^{\mathrm{BES},j} + \mu^{\mathrm{BES},j}\right)\right\} + \bar{p}^{\mathrm{SC}} \cdot \left(\gamma_y^{\mathrm{SC}} \cdot \nu^{\mathrm{SC}} + \mu^{\mathrm{SC}}\right);\ \forall y \in \mathcal{Y} \quad (6)$$

$$D_r = \sum_{\forall t \in \mathcal{T}}\left\{\tau_t \cdot \left[\lambda_r \cdot p_{r|t}^{\mathrm{G}} + \sum_{\forall j \in \mathcal{J}}\left\{10^{-3} \cdot \xi^{\mathrm{BES},j} \cdot \left(\sum_{\forall i \in \{\mathrm{ch;dch}\}}\left\{p_{r|t}^{\mathrm{BES},j,i}\right\}\right)\right\} + 10^{-3} \cdot \xi^{\mathrm{SC}} \cdot \left(\sum_{\forall i \in \{\mathrm{ch;dch}\}}\left\{p_{r|t}^{\mathrm{SC},i}\right\}\right)\right]\right\};\ \forall r \in \mathcal{R} \quad (7)$$

In (4), Φ is the vector of decision variables (see *Nomenclature*). In essence, the objective function indicates the expected cost of the storage project. While capital and yearly costs are related with the expenditures in which the project incurs due to the installation of storage components, the daily costs also include the cost of the energy acquired from the primary energy supply (AC grid). It is also worth noting how the representative roundtrips are treated in (4). As observed, the roundtrip costs are calculated for each representative roundtrip, since it is expected that energy purchased from the grid and exchanged with the system vary depending each representative set. Once these costs are calculated

for each r, they are multiplied by the total number of daily roundtrips that can be represented by this set (i.e. ω_r). This way, the calculated D_r is properly represented over a daily time horizon. Finally, these expenditures are extended to a yearly time horizon by simply multiplying them by 365.

3.3 - Mathematical models

The mathematical model of the different components involved in the studied system (see Fig. 1), are described throughout this section and incorporated to the developed MILP optimization framework as constraints.

3.3.1 - System balance

During cruise and acceleration, the traction load can be supplied by either the grid or the storage system. In contrast, the energy generated during braking can be either absorbed by the storage system or dissipated. With these considerations, the constraint (8) represents the energy balance of the system.

$$p^{\mathrm{G}}_{r|t} + \sum_{\forall j \in \mathcal{J}} \{p^{\mathrm{BES},j,\mathrm{dch}}_{r|t}\} + p^{\mathrm{SC,dch}}_{r|t} = p^{\mathrm{TW}}_{t} + p^{\mathrm{D}}_{r|t} + \sum_{\forall j \in \mathcal{J}} \{p^{\mathrm{BES},j,\mathrm{ch}}_{r|t}\} + p^{\mathrm{SC,ch}}_{r|t};\ \forall r \in \mathcal{R}, \forall t \in \mathcal{T} \quad (8)$$

3.3.2 - Grid constraints

In both wayside and on-board storage system configurations, it is realistic to assume that the power supplied from the grid is upper bounded, which is ensured by imposing the constraints (9) and (10).

$$0 \leq p^{\mathrm{G}}_{r|t} \leq \bar{p}^{\mathrm{G}};\ \forall r \in \mathcal{R}, \forall t \in \mathcal{T} \quad (9)$$

$$0 \leq p^{\mathrm{G}}_{r|t} \leq \mathbf{c}(t) \cdot \bar{p}^{\mathrm{G}};\ \forall r \in \mathcal{R}, \forall t \in \mathcal{T} \quad (10)$$

The only difference between (9) and (10) is the inclusion of the vector $\mathbf{c}(t)$. This vector is equal to 0 in catenary-less sections and 1 otherwise. In fact, the constraint (9) is applied in the case of wayside configuration. In this case, the storage system can exchange energy with the main grid regardless the availability of the catenary. On the other hand,

for on-board configurations, it is assumed that the storage system cannot be supplied from the grid during catenary-less sections. In such a case, the traction load must be covered through the HES system, which can be also charged during braking. This restriction is modelled by the constraint (10), which is applied in the case of on-board storage systems. It is worth noting that the system balance equation (8) does not vary depending on the configuration of the storage system. In the case of wayside configurations, it is simply assumed that the traction load is zero along catenary-less sections; while for on-board arrangements, the constraint (10) ensures that neither the traction load nor the storage system can be supplied from the grid if catenary is not available.

3.3.3 - Modelling the storage system

As mentioned, the storage system devoted on supplying the studied tramway installation encompasses batteries and SC banks, as customary in tramway applications [20,26]. For both storage technologies, the instantaneous power that can be exchanged is upper bounded by nominal powers [29], as said in (11) and (12).

$$0 \leq p_{r|t}^{\mathrm{BES},j,i} \leq u_{r|t}^{\mathrm{BES},j,i} \cdot \bar{p}^{\mathrm{BES},j};\ \forall i \in \{\mathrm{ch};\mathrm{dch}\}, \forall j \in \mathcal{J}, \forall r \in \mathcal{R}, \forall t \in \mathcal{T} \quad (11)$$

$$0 \leq p_{r|t}^{\mathrm{SC},i} \leq u_{r|t}^{\mathrm{SC},i} \cdot \bar{p}^{\mathrm{SC}};\ \forall i \in \{\mathrm{ch};\mathrm{dch}\}, \forall r \in \mathcal{R}, \forall t \in \mathcal{T} \quad (12)$$

In the expressions above, the product of the commitment status (binary) by the nominal power (continuous) yields a bilinear term. With the aim of preserving the MILP characterization of the optimization problem, such bilinear terms are converted to linear ones by imposing additional constraints [43]. Specifically, given a continuous variable x and a binary one δ, the following set of constraints allow to replace the product of these variables by the dummy one y.

$$x - L \cdot (1 - \delta) \leq y \leq x + L \cdot (1 - \delta) \quad (13)$$

$$-L \cdot \delta \leq y \leq L \cdot \delta \quad (14)$$

In this work, the SOC of a storage component is determined at time t by the storage status at $t-1$, and the power exchanged with the system at time t. Specifically, the energy stored in batteries is given by:

$$s_{r|t}^{\mathrm{BES},j} = s_{r|t-1}^{\mathrm{BES},j} + \tau_t \cdot \left(p_{r|t}^{\mathrm{BES},j,\mathrm{ch}} \cdot \eta^{\mathrm{BES},j,\mathrm{ch}} - \frac{p_{r|t}^{\mathrm{BES},j,\mathrm{dch}}}{\eta^{\mathrm{BES},j,\mathrm{dch}}} \right);\ \forall j \in \mathcal{J}, \forall r \in \mathcal{R}, \forall t \in \mathcal{T} \backslash t > 1 \quad (15)$$

Whereas the expression (15) is valid for batteries, the self-discharge characteristic of SCs should not be ignored. Indeed, battery technologies usually present a marginal self-discharge rate [44]. However, this characteristic may suppose up to 40 %/day of the nominal capacity in capacitors [44]. Keeping this on mind, the SOC of the SC bank at time t is defined as follows:

$$s_{r|t}^{\mathrm{SC}} = s_{r|t-1}^{\mathrm{SC}} + \tau_t \cdot \left(p_{r|t}^{\mathrm{SC,ch}} \cdot \eta^{\mathrm{SC,ch}} - \frac{p_{r|t}^{\mathrm{SC,dch}}}{\eta^{\mathrm{SC,dch}}} - \frac{\varrho^{\mathrm{SC}} \cdot Q^{\mathrm{SC}}}{24} \right);\ \forall r \in \mathcal{R}, \forall t \in \mathcal{T} \backslash t > 1 \quad (16)$$

For the both considered storage technologies, the energy stored have to lie between the nominal capacity and the DOD settings, as said the constraints (17) and (18).

$$(1 - d^{\mathrm{BES}}) \cdot Q^{\mathrm{BES},j} \leq s_{r|t}^{\mathrm{BES},j} \leq Q^{\mathrm{BES},j};\ \forall j \in \mathcal{J}, \forall r \in \mathcal{R}, \forall t \in \mathcal{T} \quad (17)$$

$$(1 - d^{\mathrm{SC}}) \cdot Q^{\mathrm{SC}} \leq s_{r|t}^{\mathrm{SC}} \leq Q^{\mathrm{SC}};\ \forall r \in \mathcal{R}, \forall t \in \mathcal{T} \quad (18)$$

It is also realistic to assume complementarity on the charging-discharging processes of the storage system, which is ensured by imposing the constraints (19) and (20).

$$\sum_{\forall i \in \{\mathrm{ch;dch}\}} \left\{ u_{r|t}^{\mathrm{BES},j,i} \right\} \leq 1;\ \forall j \in \mathcal{J}, \forall r \in \mathcal{R}, \forall t \in \mathcal{T} \quad (19)$$

$$\sum_{\forall i \in \{\mathrm{ch;dch}\}} \left\{ u_{r|t}^{\mathrm{SC},i} \right\} \leq 1;\ \forall r \in \mathcal{R}, \forall t \in \mathcal{T} \quad (20)$$

As explained in Section 2.3, time horizon representation by means of representative roundtrips assume some linking relationships among the final and initial SOCs of the different trips. Specifically, these relations are pictorially represented by green discontinuous lines in Fig. 3 and justified in Section 2.3. Mathematically, the additional set of

constraints (21) and (22) must be imposed in order to ensure a coherent representation of the SOC between representative roundtrips.

$$\begin{cases} s_{r|1}^{\mathrm{BES},j} = Q^{\mathrm{BES},j}, & \text{if } r = 1 \\ s_{r|\mathcal{T}}^{\mathrm{BES},j} = s_{1|1}^{\mathrm{BES},j}, & \text{if } r = \mathcal{R} \\ s_{r|1}^{\mathrm{BES},j} = s_{r-1|\mathcal{T}}^{\mathrm{BES},j}, & \text{if } r = \mathcal{R} \text{ or } \lambda_r \neq \lambda_{r-1} \\ s_{r|1}^{\mathrm{BES},j} = s_{r|\mathcal{T}}^{\mathrm{BES},j} = s_{r-1|\mathcal{T}}^{\mathrm{BES},j}, & \text{o.w.} \end{cases} ; \forall j \in \mathcal{J} \tag{21}$$

$$\begin{cases} s_{r|1}^{\mathrm{SC}} = Q^{\mathrm{SC}}, & \text{if } r = 1 \\ s_{r|\mathcal{T}}^{\mathrm{SC}} = s_{1|1}^{\mathrm{SC}}, & \text{if } r = \mathcal{R} \\ s_{r|1}^{\mathrm{SC}} = s_{r-1|\mathcal{T}}^{\mathrm{SC}}, & \text{if } r = \mathcal{R} \text{ or } \lambda_r \neq \lambda_{r-1} \\ s_{r|1}^{\mathrm{SC}} = s_{r|\mathcal{T}}^{\mathrm{SC}} = s_{r-1|\mathcal{T}}^{\mathrm{SC}}, & \text{o.w.} \end{cases} \tag{22}$$

One can check that the set of constraints (21) and (22) correspond with the logic cycle described in Section 2.3. Complementarily, other logical cycles can be defined for convenience by the users, which may yield other type of constraints different to those described in this paper. Therefore, the constraints (21) and (22) should be considered as guidelines in the case of further elaborations, rather than a strict rule for the application of the developed model.

It is important to note that the configuration described in Fig. 1 assumes that the storage components are connected to the tramway installation through electronic converter interfaces. This configuration is usually considered in tramway installations for ensuring a suitable voltage profile on catenary [20]. Nevertheless, the use of electronic interfaces brings additional limitations to the storage system operation. Specifically, as pointed out in [45], the response time of a storage component may be delayed up to 13 seconds due to slow response time of electronic components. In this paper, as customary for modelling slow responses of thermal generators [46], this limitation is considered by introducing artificial ramp constraints. Thus, assuming that a storage component may take z seconds to provide its rated power, a virtual ramp defined by $\Delta = 1/z$ is introduced and the following constraints are imposed.

$$-3600 \cdot \tau_{t-1} \cdot \Delta^{\mathrm{BES},j} \cdot \bar{p}^{\mathrm{BES},j} \leq p_{r|t}^{\mathrm{BES},j,i} - p_{r|t-1}^{\mathrm{BES},j,i} \leq 3600 \cdot \tau_{t-1} \cdot \Delta^{\mathrm{BES},j} \cdot \bar{p}^{\mathrm{BES},j};\ \forall i \in \{\mathrm{ch};\mathrm{dch}\}, \forall j \in \mathcal{J}, \forall r \in \mathcal{R}, \forall t \in \mathcal{T} \backslash t > 1 \quad (23)$$

$$-3600 \cdot \tau_{t-1} \cdot \Delta^{\mathrm{SC}} \cdot \bar{p}^{\mathrm{SC}} \leq p_{r|t}^{\mathrm{SC},i} - p_{r|t-1}^{\mathrm{SC},i} \leq 3600 \cdot \tau_{t-1} \cdot \Delta^{\mathrm{SC}} \cdot \bar{p}^{\mathrm{SC}};\ \forall i \in \{\mathrm{ch};\mathrm{dch}\}, \forall r \in \mathcal{R}, \forall t \in \mathcal{T} \backslash t > 1 \quad (24)$$

Finally, it is worth considering limits on the nominal power of storage system. This factor is determined by the installed capacity and the energy-to-power ratio [29, 42], which varies depending on the storage technology or manufacturer. In this regard, it is assumed that each storage technology may be described by a minimum value of the energy-to-power ratio. Thereby, the following bounds are imposed on the rated power of batteries and SC.

$$0 \leq \bar{p}^{\mathrm{BES},j} \leq \frac{Q^{\mathrm{BES},j}}{\underline{\vartheta}^{\mathrm{BES},j}};\ \forall j \in \mathcal{J} \quad (25)$$

$$0 \leq \bar{p}^{\mathrm{SC}} \leq \frac{Q^{\mathrm{SC}}}{\underline{\vartheta}^{\mathrm{SC}}} \quad (26)$$

By (25) and (26), the rated power of storage assets may vary from zero to a determined threshold fixed by a minimum characteristic energy-to-power ratio. Therefore, nominal capacity and power are linked, as occurred in real storage facilities. In this way, the approach adopted in this paper is equivalent to consider the energy-to-power ratio a variable of the problem.

3.3.5 - Project limits

Frequently, additional limitations are imposed by owners or environmental conditions. For instance, the capital costs of the storage project are limited by a self-imposed budget limit that the investors are not willing or allowed to exceed [24]. This condition is expressed by the constraint (27).

$$K \leq \Psi \quad (27)$$

Also, total storage capacity of the different components may be limited due to unavailability of proper infrastructure, space limitations or environmental concerns [47, 48]. This restraint is modelled by the constraints (28) and (29).

$$\sum_{\forall j \in \mathcal{J}} \{Q^{\mathrm{BES},j}\} \leq \overline{Q}^{\mathrm{BES}} \tag{28}$$

$$Q^{\mathrm{SC}} \leq \overline{Q}^{\mathrm{SC}} \tag{29}$$

Oftentimes, the total weight of the storage bank is bounded to avoid impairing the performance of the traction machinery or even for security reasons [23]. In storage applications, the energy density gives an idea of the quantity of energy can be accumulated by unit of mass for a given storage technology [44]. In this sense, the weight restriction imposed on the storage system can be modelled as follows:

$$\sum_{\forall j \in \mathcal{J}} \left\{ \frac{10^3 \cdot Q^{\mathrm{BES},j}}{\rho^{\mathrm{BES},j}} \right\} + \frac{10^3 \cdot Q^{\mathrm{SC}}}{\rho^{\mathrm{SC}}} \leq \mathrm{M} \tag{30}$$

4 - Case study

Throughout this section, the developed approach is validated through different simulations and illustrative results. A real tramway installation placed at Cuenca - Ecuador, has been selected as benchmark, which is described in Section 4.1. The results are presented for the two studied storage configurations, i.e. wayside and on-board. The developed MILP optimization model described in Section 3 has been coded under Matlab environment and solved with Gurobi [49]. Although the results presented in this section were obtained from a particular real installation, they serve to validate the developed approach, proving its universal applicability.

4.1 - System description and input data

The tramway under study connects 27 stations across the city in a north-south direction. The length of the round trip is 20.4 km and is completed in approximately 73 minutes. Currently, this tramway is supplied through substations located along the route

at 750 Vdc. The tramway route is shown in Fig. 6 (a), the slope during each journey is shown in Fig. 6 (b).

Real measurements of the traction load during a roundtrip are available for the installation under study (this parameter can be also obtained from the well-known power-speed curves [20]). The measured data is available with a resolution of 1 second, which results in 4,341 sample points in total for a unique roundtrip. To reduce the amount of data to be treated, the APCA representation of the measured samples is taken, such as explained in Section 2.4. Table 1 presents various indicative indexes (e.g. see [50] for a further explanation about such indicators) using two thresholding approximations [40, 41]. As seen, by using the APCA approximation, the total data can be reduced to 310 or 624 samples applying a universal or sub-band thresholding, respectively. Although the application of the universal thresholding technique yields a further reduced data sampling, more accurate results are obtained with the sub-band specific thresholding approach, reason why the latter has been chosen for simulations. Fig. 6 (c) plots the traction load of the installation under study and its corresponding APCA representation with sub-band thresholding.

Table 1 - Some evaluation indexes of the APCA representation of the original data with two thresholding approaches

Index	Universal thresh. [40]	Sub-band thresh. [41]
Samples	310	624
MAE	28.51 %	4.59 %
RMSE	54.60 %	12.51 %

It is worth mentioning the MILP framework described in Section 3 was run with the original measured data with high resolution and using APCA representation with Sub-band thresholding. In the former case, the simulations took various hours on average,

while the computational time was reduced to 10-20 minutes applying data reduction techniques. Also, results obtained did not only differ substantially, and only marginal differences were observed that have not a significant impact in real applications.

Currently, the considered tramway completes 15 roundtrips through a day. Two pricing rates have been considered for simulations. On the one hand, a flat pricing scheme with energy cost equal to 0.12 $/kWh has been taken (scenario A). On the other hand, a common time of use mechanism has been chosen in which the energy cost takes 0.09 $/kWh and 0.16 $/kWh during off-peak and peak hours, respectively (scenario B). Table 2 provides a schematic summary of the trip distribution through a day, energy cost during each roundtrip and representation by means of representative roundtrips for the trip scheduling of the considered installation.

Three mature battery technologies have been considered in simulations, whose different costs and characteristics are collected in Table 3. Different storage layouts have been analysed. Firstly, the so-called base case in which the system is lonely supplied through the main grid is considered (configuration 1). Secondly, the system encompasses a storage system only comprising a SC bank (configuration 2). And thirdly, a hybrid storage system with SC and BES is considered (configuration 3). Other required parameters have been chosen adequately for the purposes of this research and are reported in Table 4.

Table 2 - Schematic view of the approach considered for representing the daily trip scheduling of the tramway installation under study

Pricing rate	Trip #														
	1	2	3	4	5	6	7	8	9	10	11	12	13	14	15
A	*r = 1*	*r = 2*	*r = 2*	*r = 2*	*r = 2*	*r = 2*	*r = 2*	*r = 2*	*r = 2*	*r = 2*	*r = 2*	*r = 2*	*r = 2*	*r = 2*	*r = 3*
B	*r = 1*	*r = 2*	*r = 2*	*r = 2*	*r = 2*	*r = 3*	*r = 4*	*r = 4*	*r = 4*	*r = 4*	*r = 4*	*r = 4*	*r = 4*	*r = 4*	*r = 5*
Off-peak (0.09 $/kWh)							Peak (0.16 $/kWh)								

(a)

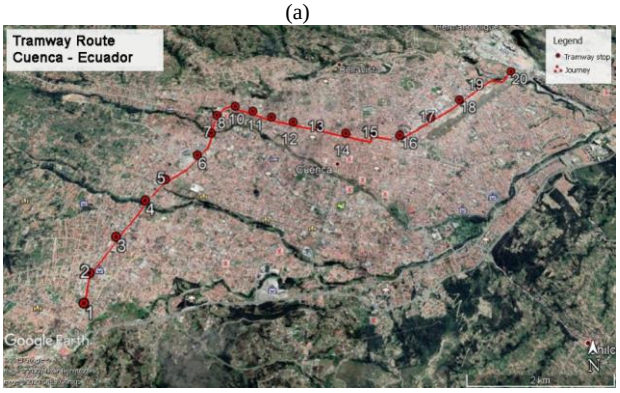

(b)

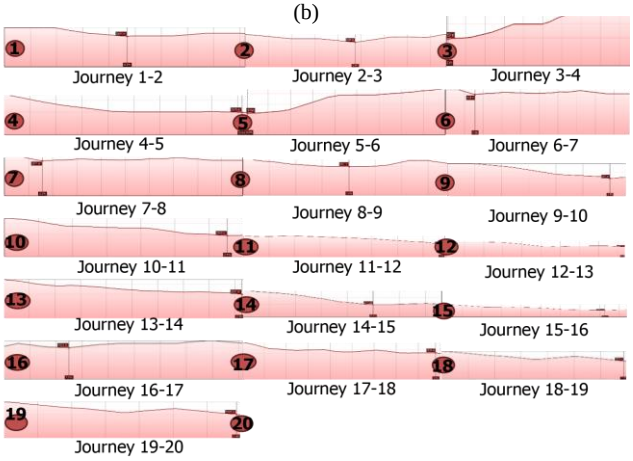

(c)

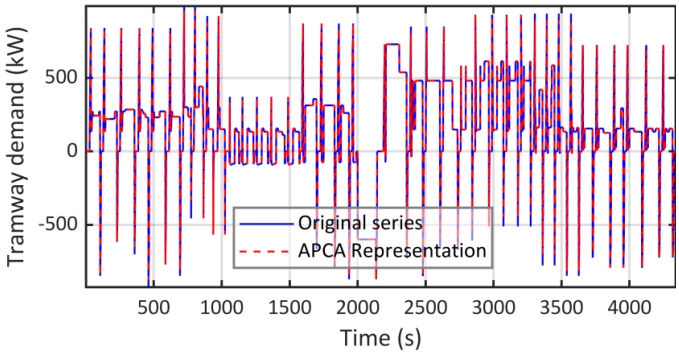

Fig. 6 - Characteristics of the studied tramway installation. (a) Tramway route in the city of Cuenca - Ecuador; (b) Slopes during tramway journey; (c) Measured traction load and its corresponding APCA representation using sub-band thresholding

Table 3 - Characteristics of different storage technologies contemplated in the case study [44, 45]

Feature	Lead-Acid	NiCd	Li-ion	SC
Estimated lifetime (years)	10	15	10	15
Charging/discharging efficiency (%)	80	70	95	90
Min. Energy-to-power ratio (hrs)	1.50	2	1.50	0.0125
Energy density (Wh/kg)	40	100	250	20
Self-discharge rate (pu-day)	--	--	--	0.25
Δ (pu)	0.20	0.20	0.20	1
Costs				
Capital ($/kWh)	747.78	943.80	962.00	765.00
Fixed O&M ($/kW)	4.11	13.31	8.35	1.00
Variable O&M ($/MWh)	0.45	0.61	2.54	0.30
Replacement ($/kW)	208.12	635.25	446.50	9.56
Power conversion system ($/kW)	562.65	289.20	560.23	229.00

Table 4 - Other parameters considered in simulations

Parameter	Value
Max. power that can be purchased from the grid	1,000 kW
DOD	0.30
Estimated project lifetime	30 years
Inflation rate	1.0027

4.2 - Wayside configuration

The first experiments are devoted on designing a wayside storage system for the tram-way installation under study. For such case, $\overline{Q}^{\mathrm{SC}} = 5$ kWh, $\overline{Q}^{\mathrm{BES}} = 100$ kWh and $\Psi = 250{,}000$ $ have been taken. Table 5 shows the total project cost and storage system layout obtained for this configuration. As observed, the value of the objective function is drastically reduced when a storage system is installed. The project cost is amenably higher with the pricing rate B, which is logic since more roundtrips are completed during peak hours. In all cases, the SC bank has been sized at 5 kWh, which supposes its maximum allowed capacity. Capacity of the battery bank is largely provided by Li-ion batteries (~56-61 %),

while the other technologies contribute with less capacity up to reach 100 kWh altogether for all studied scenarios. These results were expected since while the SC shows a very high rated power (due to a very low energy-to-power ratio), the Li-ion technology presents, by far, the highest efficiency. This way, the resulted layout is considered optimal to effectively obtain a coordination of the different storage technologies. In all cases, the rated power was determined to be the maximum allowed for all storage technologies (i.e. the minimum energy-to-power ratio). This result is quite logic taking into account that costs derived from nominal power of storage assets are easily compensated by monetary savings obtained from reducing the energy purchased from the grid.

As seen, the storage layout is designed so that the maximum power of the assets is maximized. In this sense, SC is sized at its maximum allowed capacity to properly cover peak demands. For the batteries, the algorithm attends to other aspects such as efficiency and related costs, but in all cases the rated power was also sized at maximum allowed values. This way, high peak demand can be covered by the HES, avoiding large consumptions be supplied from the grid incurring in very high energy costs. Similarly, high power rates allow to exploit peak power generation during braking, which is stored and can be used to further reduce the energy demand from the main grid. These results follow logic ideas which leads to conclude that the developed methodology provides accurate results with very low computational burden as drawn in the previous section.

Table 5 - Project cost and storage system layout with wayside configuration

Config. #	Energy pricing rate	Project cost ($)	SC	Lead-acid	NiCd	Li-ion
1	A	5,190,400	--	--	--	--
2	A	1,829,700	5.00 kWh 400 kW	--	--	--
3	A	1,460,100	5.00 kWh 400 kW	16.59 kWh 11.06 kW	22.11 kWh 11.06 kW	61.30 kWh 40.87 kW
1	B	5,709,400	--	--	--	--
2	B	2,026,300	5.00 kWh 400 kW	--	--	--
3	B	1,668,200	5.00 kWh 400 kW	18.75 kWh 9.38 kW	25.00 kWh 12.50 kW	56.25 kWh 37.50 kW

The developed methodology is versatile enough to not only provide the storage layout, but also other useful results that may be valuable in planning stages. As a sake of example, Table 6 provides some valuable results for the wayside configuration. As seen, the total energy purchased from the grid (and consequently the total energy cost) through the project lifetime are further reduced as more storage facilities and technologies are deployed. As expected, the total energy dissipated in the braking resistor is also minimized by installing SC and battery banks, which is logic since the tramway installation necessarily dissipates all the energy generated during braking if no storage is considered. These results are better illustrated in Fig. 7, where the power balance during an acceleration-cruise-braking cycle with the storage configuration 3 and energy pricing rate A is plotted. As appreciated in this figure, most of the traction load is supplied through the SC bank which, is capable to cover peak power demands; in contrast, the BES system enables large storage capacity. In this case, the energy demanded during acceleration (peak demand), is largely supplied through the storage system, which takes advantage of the energy generated during braking to be partially charged. This way, the energy purchased from the grid and dissipated in the braking resistor are minimized. The results in Fig. 7 also explains how the storage system helps to notably reduce the project cost. Indeed, one can see that peak load is almost fully supplied from storage assets. In tramway applications, peak consumptions may reach very high values (~1,000 kW for our case). These peak loads, although have very short duration, provoke high energy demands which are

reflected in very high energy costs. The results and explanation above strengthens the validation of the developed methodology, which has demonstrated not only its accurateness, but also the amount of valuable results that may be extracted with the developed framework, which supposes a salient feature in comparison with other approaches.

Table 6 - Some indicative results obtained with wayside configuration through the estimated project lifetime

Config. #	Energy pricing rate	Total energy purchased from the grid (MWh)	Total energy dissipated (MWh)	Total energy cost ($)
1	A	1,386.10	314.66	5,190,400
2	A	454.91	198.40	1,703,400
3	A	298.65	174.61	1,118,300
1	B	1,386.10	314.66	5,709,400
2	B	461.26	177.10	1,899,900
3	B	322.71	156.91	1,330,100

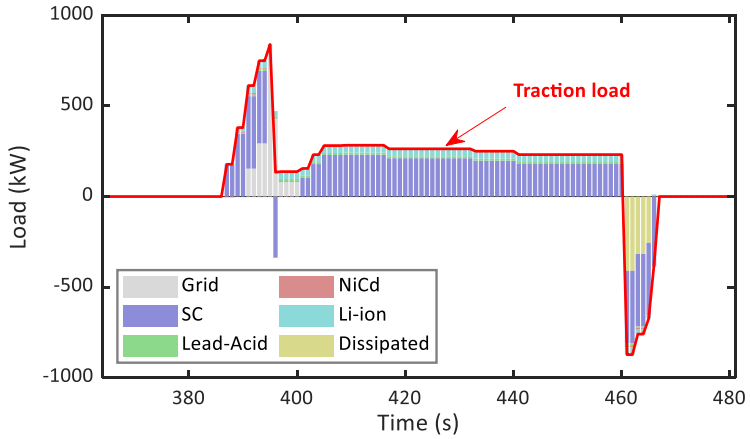

Fig. 7 - Power balance during an acceleration-cruise-braking cycle with wayside storage system for the configuration 3 and energy pricing rate A. In this figure, negative values indicate charging and dissipated powers

To further illustrate the developed mathematical solution approach, Fig. 8 plots the state of charge of the Li-ion batteries for a complete day with configuration 3 and energy pricing rate B. As observed, the rules imposed in (21) and (22) are properly matched. Indeed, the state of charge at the beginning of a roundtrip is equal to the charging at the end of the roundtrip. This behaviour changes during the initial and final roundtrips and at those moments in which the energy pricing rate changes. In such cases, one can check

that rules (21) and (22) are also accomplished. This way, the state of charge of the different assets is kept coherent among consecutive roundtrips, without needing calculating each one separately, which is reflected in a light computational burden of the whole procedure. It is also worth noting in Fig. 8 that batteries are very few discharged (only ~5% of the total capacity). This demonstrates that batteries are more devoted on providing large and long-term capacity rather than quick responses and high power rate. This way, the batteries are perfectly complemented with the SC bank. This aspect is better illustrated by the results in Table 7. Here, the expected total energy exchanged with the system of each storage technology is reported. As seen, the SC bank is more profusely exploited than the batteries. This result is propitiated by low energy-to-power ratio and fast response of the SC in comparison with BES. In this regard, capacitor storage technology is able to supply and absorb more energy and more quickly than the other storage devices. Comparing the different battery technologies, it is clear than the more installed capacity, the more energy is exchanged, which results coherent.

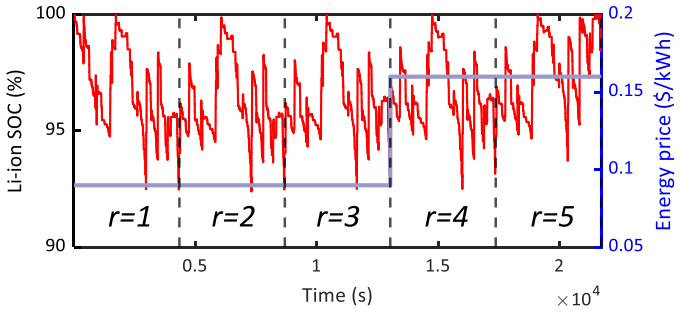

Fig. 8 - State of charge of the SC throughout a complete day with energy pricing scheme B and configuration 3

Table 7 - Expected total energy exchanged with the tramway system through the estimated project lifetime

Config. #	Energy pricing rate	SC (MWh)	Lead-acid (MWh)	NiCd (MWh)	Li-ion (MWh)
3	A	32,489.25	1,485.30	3,069.50	5,605.20
3	B	31,997.16	1,688.20	3,203.10	4,928.20

4.3 - On-board configuration

Now, let us analyse the case in which the storage facilities are installed on-board. To better illustrate this situation, two catenary-less sections throughout the tramway route are considered. For this case, $\overline{Q}^{\mathrm{SC}} = 5$ kWh, $\overline{Q}^{\mathrm{BES}} = 5$ kWh, $\Psi = 250{,}000$ \$ and $\mathrm{M} = 300$ kg have been taken. Table 8 is analogue to Table 5 for the on-board configuration. In these circumstances, the problem was only feasible with the storage configuration 3. This result was expected since the SC bank is not capable to lonely supply the traction load through catenary-less sections and, therefore, batteries are necessary to complement the storage capacity of capacitors. For this configuration, the imposed weight becomes a crucial aspect to design the storage system. In such case, a trade-off among cost, energy density, efficiency and lifetime is searched. This is the reason why the BES layout is uniquely formed by NiCd batteries. As occurred in the wayside configuration, the rated power of the different assets took the maximum allowed value in all cases. These results are coherent follow the same logic that in the case of wayside configuration, thus serving to further validate the developed approach.

Table 8 - Project cost and storage system layout with on-board configuration

Config. #	Energy pricing rate	Project cost ($)	SC	Lead-acid	NiCd	Li-ion
1	A			Infeasible		
2	A			Infeasible		
3	A	1,796,100	5.00 kWh 400 kW	0.00 kWh 0.00 kW	5.00 kWh 2.50 kW	0.00 kWh 0.00 kW
1	B			Infeasible		
2	B			Infeasible		
3	B	1,961,500	5.00 kWh 400 kW	0.00 kWh 0.00 kW	5.00 kWh 2.50 kW	0.00 kWh 0.00 kW

Fig. 9 depicts the scheduling result for a characteristic catenary less tram with configuration 3 and pricing rate A. As observed in this figure, traction load is mostly supplied from the SC bank during cruise, while the batteries are unable to cover high consumptions due to its limited rated power and capacity; thus, this technology is mainly focused on supporting the operation of SCs. In this figure it can be also appreciated that braking energy is largely stored instead of dissipating. This last point is better illustrated in Fig. 9

(b), where the SOC of the SC and BES system for the same section of Fig. 9 (a) is plotted. As seen, the SC bank is much further exploited than the BES system, which only provides residual storage capacity during cruise. The SOC of the SC falls almost its minimum capacity during cruise along the catenary-less section, while the energy generated during braking is destined to recover its SOC as much as possible (the SC works at its rated power during braking), while the surplus energy has to be inevitably dissipated.

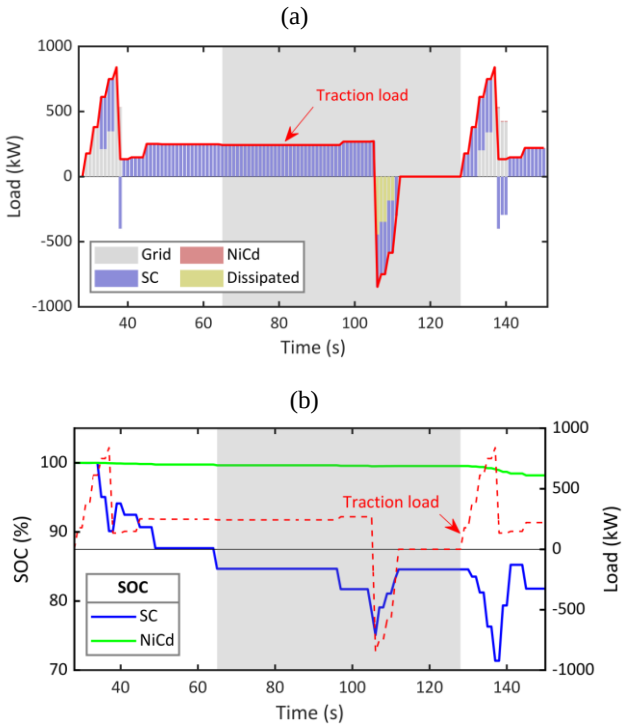

Fig. 9 - (a) Power balance during a catenary-less section (denoted by grey shaded area) with on-board storage system for the configuration 3 and energy pricing rate A. In this figure, negative values indicate charging and dissipated powers; (b) SOC of the storage system during a catenary-less section (denoted by grey shaded area) with on-board storage system for the configuration 3 and energy pricing rate A

4.4 - Comparison of wayside and on-board configurations

In this paper, results for two typical storage configurations for tramway applications, namely wayside and on-board, have been provided. This supposes one of the most salient features of the developed methodology, which is versatile enough to be adapted to different configurations and thus comparing different constructive solutions. Table 9 is a summary of some indicative values obtained with both configurations. Since the on-board configuration resulted unfeasible without batteries, only the layouts including BES are

compared. As observed, the estimated project cost is lower in the case of wayside configuration. This is logic because with this configuration capacity of batteries is much larger. In this sense, the maximum weight imposed in the storage system suppose an important barrier in the case of the on-board configuration.

It is also worth noting that more energy is purchased from the grid in the case of on-board configuration, despite that in this scenario the tramway cannot be supplied from the grid along catenary-less stretches. However, due to storage systems are further exploited in this case, more energy has to be purchased from the grid in order to recover the SOC of the storage facilities during cruise under catenary. It can be also observed that more energy is dissipated in the braking resistance. This result is also explained by the limited capacity of on-board storage facilities, which limits the capacity of the system to store the energy generated during braking.

Table 9 - Summary of results obtained with wayside and on-board installations. Only results for configuration 3 are included

Config.		Expected project cost ($)	Total energy purchased from the grid (MWh)	Total energy dissipated (MWh)	Total energy cost ($)
Wayside	3-A	1,460,100	298.65	174.61	1,118,300
	3-B	1,668,200	322.71	156.91	1,330,100
On-board	3-A	1,796,100	443.14	197.25	1,659,341
	3-B	1,961,500	442.87	175.76	1,824,711

5 - Conclusions and future works

A methodology for planning HES systems for tramway applications has been developed. The developed framework is formulated as a MILP problem and allows to contemplate different storage facilities such as super-capacitors and different batteries technologies. To reduce the intrinsic high dimensional resolution of the tramway measured data, representative one-day trip selection approaches alongside APCA dimensionality reduction techniques have been applied, which allow to easily consider dynamic energy pricing

schemes. Different components aging are also considered, thus obtaining an accurate but tractable yet mathematical procedure.

In this way, different systems configurations, layouts and pricing scenarios have been compared for a real tramway installation. In this case study, the developed framework was capable to calculate the different storage capacities and nominal powers with accurateness. In addition, because its versatility, the developed mathematical tool allowed to obtain various relevant results. For example, it has been shown that the total project cost may be reduced by 71% with respect to the base case in which storage capability is not contemplated. Storage facilities also enable a better exploitation of the energy braking, which can be stored rather than dissipated. This capability allows to reduce the energy acquired from the grid and, consequently, the energy costs through the project lifetime are minimized. Also, interaction of the different storage facilities has been highlighted. Thus, while super-capacitors are useful to handle fast peak consumptions, batteries mostly provide large and long-term storage capacity but limited power supply. Wayside and on-board configurations have been compared, showing that restrictions in the total weight of the HES system suppose a formidable barrier in on-board configurations. This bound limits the total capacity installed, thus incrementing the project costs compared with the wayside layout.

Future works should be focused on developing control strategies for HES systems besides applying similar procedures for sizing hybrid energy systems based on renewable generators for tramway applications.

6 - Acknowledgments

The icons used in the figures of this paper were created by Freepik, Smashicons and Pixel perfect, from www.flaticon.com

7 – References

[1] M. Ceraolo, G. Lutzemberger. Stationary and on-board storage systems to enhance energy and cost efficiency of tramways. *Journal of Power Sources* 2014; 264: 128-139. 10.1016/j.jpowsour.2014.04.070.

[2] V.I. Herrera, A. Milo, H. Gaztañaga, I. Etxeberria-Otadui, I. Villarreal, H. Camblong. Adaptive energy management strategy and optimal sizing applied on a battery-supercapacitor based tramway. *Applied Energy* 2016; 169: 831-845. 10.1016/J.APENERGY.2016.02.079.

[3] V.I. Herrera, H. Gaztanaga, A. Milo, A. Saez-de-Ibarra, I. Etxeberria-Otadui, T. Nieva. Optimal Energy Management and Sizing of a Battery-Supercapacitor-Based Light Rail Vehicle With a Multiobjective Approach. *IEEE Transactions on Industry Applications* 2016; 52(4): 3367-3377. 10.1109/TIA.2016.2555790.

[4] J. Kim, Y. Suharto, T.U. Daim. Evaluation of Electrical Energy Storage (EES) technologies for renewable energy: A case from the US Pacific Northwest. *Journal of Energy Storage* 2017; 11: 25-54. 10.1016/j.est.2017.01.003.

[5] J. Figgener, et al. The development of stationary battery storage systems in Germany - A market review. *Journal of Energy Storage* 2020; 29: 101153. 10.1016/j.est.2019.101153.

[6] M. Arbabzadeh, G.M. Lewis, G.A. Keoleian. Green principles for responsible battery management in mobile applications. *Journal of Energy Storage* 2019; 24: 100779. 10.1016/j.est.2019.100779.

[7] Y. Hu, T.S. Fisher. Suggested standards for reporting power and energy density in supercapacitor research. Bulletin of Materials Science 2018; 41: 124. 10.1007/S12034-018-1641-Z.

[8] W.D. Sheers. Electrical equipment of battery road vehicles. *Proceedings of the IEE - Part II Power Engineering* 1952; 99: 457-464. 10.1049/PI-2.1952.0108.

[9] P. Radcliffe, J.S. Wallace, L.H. Shu. Stationary applications of energy storage technologies for transit systems. In: *2010 IEEE Electric Power Energy Conference*, Halifax, NS, Canada, 2010. 10.1109/EPEC.2010.5697222.

[10] A.S. Al-Sumaiti, M. Salama, M. El-Moursi, T.S. Alsumaiti, M. Marzband. Enabling electricity access: revisiting load models for AC-grid operation - Part I. *IET Generation Transmission & Distribution* 2019; 13: 2563-2571. 10.1049/IET-GTD.2018.5556.

[11] A.S. Al-Sumaiti, M. Salama, M. El-Moursi, T.S. Alsumaiti, M. Marzband. Enabling electricity access: a comprehensive energy efficient approach mitigating climate/weather variability – Part II. *IET Generation Transmission & Distribution* 2019; 13: 2572-2583. 10.1049/IET-GTD.2018.6413.

[12] L. Cheng, P. Acuna, R.P. Aguilera, J. Jiang, J. Flecther, C. Baier. Model predictive control for Energy Management of a hybrid energy storage system in Light Rail Vehicles. In: *2017 11th IEEE Int. Conf. Compat. Power Electron. Power Eng. CPE-Powereng*, Cádiz, Spain, 2017: 683–688. 10.1109/CPE.2017.7915255.

[13] V. I. Herrera, H. Gaztanga, A. Milo, T. Nieva and I. Etxeberria-Otadui. Optimal Operation Mode Control and Sizing of a Battery-Supercapacitor Based Tramway. In: *2015 IEEE Vehicle Power and Propulsion Conference (VPPC)*, Montreal, Canada, 2015: 1-6. 10.1109/VPPC.2015.7352988.

[14] M. Ceraolo, G. Lutzemberger, E. Meli, L. Pugi, A. Rindi, G. Pancari. Energy storage systems to exploit regenerative braking in DC railway systems: Different approaches to improve efficiency of modern high-speed trains. Journal of Energy Storage 2018; 16: 269-279. 10.1016/j.est.2018.01.017.

[15] M. Ceraolo, R. Giglioli, G. Lutzemberger, A. Bechini. Cost effective storage for energy saving in feeding systems of tramways. In: *2014 IEEE International Electric Vehicle Conference (IEVC)*, Florence, Italy, 2014: 1-6. 10.1109/IEVC.2014.7056112.

[16] J. Yang, X. Xu, Y. Peng, J. Zhang, P. Song. Modeling and optimal energy management strategy for a catenary-battery-ultracapacitor based hybrid tramway. *Energy* 2019; 183: 1123-1135. 10.1016/j.energy.2019.07.010.

[17] P. García, L.M. Fernández, J.P. Torreglosa, F. Jurado. Operation mode control of a hybrid power system based on fuel cell/battery/ultracapacitor for an electric tramway. *Computers & Electrical Engineering* 2013; 39: 1993-2004. 10.1016/j.compeleceng.2013.04.022.

[18] J.P. Torreglosa, P. Garcia, L.M. Fernandez, F. Jurado. Predictive control for the energy management of a fuel-cell-battery- supercapacitor tramway. *IEEE Transactions on Industrial Informatics* 2014; 10(1): 276-285. 10.1109/TII.2013.2245140.

[19] Q. Li, T. Wang, C. Dai, W. Chen, L. Ma. Power Management Strategy Based on Adaptive Droop Control for a Fuel Cell-Battery-Supercapacitor Hybrid Tramway. *IEEE Transactions on Vehicular Technology* 2018; 67: 5658-5670. 10.1109/TVT.2017.2715178.

[20] Y. Han, Q. Li, T. Wang, W. Chen, L. Ma. Multisource coordination energy management strategy based on SOC consensus for a PEMFC-battery-supercapacitor hybrid tramway. *IEEE Transactions on Vehicular Technology* 2018; 67(1): 296-305. 10.1109/TVT.2017.2747135.

[21] Y. Han, N. Cao, Z. Hong, Q. Li, W. Chen. Experimental Study on Energy Management Strategy for Fuel Cell Hybrid Tramway. In: *2016 IEEE Vehicle Power and Propulsion Conference (VPPC)*, Hangzhou, China, 2016: 1-6. 10.1109/VPPC.2016.7791686.

[22] F. Ciccarelli, D. Iannuzzi, K. Kondo, L. Fratelli. Line-Voltage Control Based on Wayside Energy Storage Systems for Tramway Networks. *IEEE Transactions on Power Electronics* 2016; 31(1): 884-899. doi.org/10.1109/TPEL.2015.2411996.

[23] F. Peng, et al. Development of master-slave energy management strategy based on fuzzy logic hysteresis state machine and differential power processing compensation for a PEMFC-LIB-SC hybrid tramway. *Applied Energy* 2017; 206: 346-363. 10.1016/j.apenergy.2017.08.128.

[24] M. Tostado-Véliz, D. Icaza-Alvarez, F. Jurado. A novel methodology for optimal sizing photovoltaic-battery systems in smart homes considering grid outages and demand response. *Renewable Energy* 2021; 170: 884-896. 10.1016/j.renene.2021.02.006.

[25] M. Hemmati, et al. Economic-environmental analysis of combined heat and power-based reconfigurable microgrid integrated with multiple energy storage and demand response program. *Sustainable Cities & Society* 2021; 69: 102790. 10.1016/J.SCS.2021.102790.

[26] A. Ghasemi, H. Jamshidi Monfared, A. Loni, M. Marzband. CVaR-based retail electricity pricing in day-ahead scheduling of microgrids. *Energy* 2021; 227: 120529. 10.1016/J.ENERGY.2021.120529.

[27] N. Gholizadeh, M. Abedi, H. Nafisi, M. Marzband, A. Loni, G. A. Putrus. Fair-Optimal Bilevel Transactive Energy Management for Community of Microgrids. *IEEE Systems Journal* 2021 (Early Access). 10.1109/JSYST.2021.3066423.

[28] M.A. Mirzaei, et al. Network-Constrained Joint Energy and Flexible Ramping Reserve Market Clearing of Power- and Heat-Based Energy Systems: A Two-Stage Hybrid IGDT-Stochastic Framework. *IEEE Systems Journal* 2021; 15(2): 1547-1556. 10.1109/JSYST.2020.2996952.

[29] I. Alsaidan, A. Khodaei, W. Gao. A Comprehensive Battery Energy Storage Optimal Sizing Model for Microgrid Applications. *IEEE Transactions on Power Systems* 2018; 33(4): 3968-3980. 10.1109/TPWRS.2017.2769639.

[30] N.G. Paterakis, O. Erdinç, A.G. Bakirtzis, J.P.S. Catalão. Optimal household appliances scheduling under day-ahead pricing and load-shaping demand response strategies. *IEEE Transactions on Industrial Informatics* 2015; 11(6): 1509-1519. 10.1109/TII.2015.2438534.

[31] M. Tostado-Véliz, P. Arévalo, F. Jurado. A comprehensive electrical-gas-hydrogen Microgrid model for energy management applications. *Energy Conversion & Management* 2021; 228: 113726. 10.1016/j.enconman.2020.113726.

[32] D. Setlhaolo, X. Xia, J. Zhang. Optimal scheduling of household appliances for demand response. *Electric Power Systems Research* 2014; 116: 24-28. 10.1016/j.epsr.2014.04.012.

[33] P. Arévalo, A. Cano, J. Benavides, F. Jurado. Feasibility study of a renewable system (PV/HKT/GB) for hybrid tramway based on fuel cell and super capacitor. *IET Renewable Power Generation* 2021; 15: 491-503. 10.1049/rpg2.12056.

[34] M. Masih-Tehrani, M.R. Ha'iri-Yazdi, V. Esfahanian, A. Safaei. Optimum sizing and optimum energy management of a hybrid energy storage system for lithium battery life improvement. *Journal of Power Sources* 2013; 244: 2-10. 10.1016/j.jpowsour.2013.04.154.

[35] B.-K Yi, C. Faloutsos. Fast Time Sequence Indexing for Arbitrary Lp Norms. In: Proceedings of the 26th International Conference on Very Large Databases, Cairo, Egypt, 2000.

[36] E. Keogh, K. Chakrabarti, M. Pazzani, S. Mehrotra. Dimensionality Reduction for Fast Similarity Search in Large Time Series Databases. *Knowledge & Information Systems* 2001; 3: 263-286. 10.1007/pl00011669.

[37] C. Faloutsos, H. V. Jagadish, A.O. Mendelzon, T. Milo. Signature technique for similarity-based queries. In: *Proceedings of theCompression and Complexity of SEQUENCES 1997*; Positano, Italy, 1997: 2-20. 10.1109/sequen.1997.666899.

[38] K. Chakrabarti, E. Keogh, S. Mehrotra, M. Pazzani. Locally Adaptive Dimensionality Reduction for Indexing Large Time Series Databases. *ACM Transactions on Database Systems* 2002; 27: 188-228. 10.1145/568518.568520.

[39] J. Morse. Matlab code for denoising and compression of time series data using Adaptive Piecewise Constant Approximation, 2018. https://github.com/Jcmorse/APCA (accessed April 10, 2021).

[40] D.L. Donoho, I.M. Johnstone. Ideal Spatial Adaptation by Wavelet Shrinkage. Biometrika 1994; 81: 425-55. 10.2307/2337118

[41] S.G. Chang, B. Yu, M. Vetterli. Adaptive wavelet thresholding for image denoising and compression. *IEEE Transactions on Image Processing* 2000; 9(9): 1532-1546. 10.1109/83.862633.

[42] P. Arévalo, M. Tostado-Véliz, F. Jurado. A novel methodology for comprehensive planning of battery storage systems. *Journal of Energy Storage* 2021; 37: 102456. 10.1016/j.est.2021.102456.

[43] A. Gupte, S. Ahmed, M.S. Cheon, S. Dey. Solving mixed integer bilinear problems using MILP formulations. *SIAM Journal on Optimization* 2013; 23: 721-744. 10.1137/110836183.

[44] B. Zakeri, S. Syri. Electrical energy storage systems: A comparative life cycle cost analysis. *Renewable & Sustainable Energy Reviews* 2015; 42: 569-596. 10.1016/j.rser.2014.10.011.

[45] K. Mongird, et al. Energy Storage Technology and Cost Characterization Report. Hydro Wires. U.S. Dpt. Of Energy, Rep. No: PNNL-28866, 2019. https://energystorage.pnnl.gov/pdf/PNNL-28866.pdf (accessed April 10, 2021).

[46] B. Zhao, A.J. Conejo, R. Sioshansi. Unit commitment under gas-supply uncertainty and gas-price variability. *IEEE Transactions on Power Systems* 2017; 32(3): 2394-2405. 10.1109/TPWRS.2016.2602659.

[47] D. Sauer D, G. Fuchs, B. Lunz, M. Leuthold. Technology Overview on Electricity Storage: Overview on the potential and on the deployment perspectives of electricity storage technologies. RWTH Aachen University, 2021. 10.13140/RG.2.1.5191.5925.

[48] T.M. Gür. Review of electrical energy storage technologies, materials and systems: Challenges and prospects for large-scale grid storage. *Energy & Environmental Science* 2018; 11: 2696-2767. 10.1039/c8ee01419a.

[49] Gurobi - The fastest solver. https://www.gurobi.com/ (accessed April 10, 2021).

[50] G.A. Rob J. Hyndman. *Forecasting: principles and practice. 3rd edition*. OTexts, Melbourne, Australia, 2021. OTexts.com/fpp3 (accessed April 10, 2021).